ELSEVIER

PII: S0032-3861(96)00018-9

Polymer Vol. 38 No. 19, pp. 4881–4889, 1997

0032-3861/97/$17.00 + 0.00

Curie transition, ferroelectric crystal structure and ferroelectricity of a VDF/TrFE (75/25) copolymer: 2. The effect of poling on Curie transition and ferroelectric crystal structure

Kap Jin Kim* and Gwan Bum Kim†

Department of Textile Engineering, College of Engineering, Kyung Hee University, 1 Seochun-ri, Kiheung-eup, Yongin-si, Kyunggi-do 449-701, South Korea

(Received 12 April 1996; revised 24 October 1996)

Three typical 75/25 VDF/TrFE copolymer samples, differing in the amounts of the three kinds of ferroelectric phases of different thermodynamic stability in the ferroelectric state, were prepared by consecutive annealing below the Curie transition point and were then poled at a field strength of 0.9 MV cm^{-1}. New findings were made based on d.s.c., X-ray diffraction, i.r. spectroscopy and Raman scattering results of the poled samples. D.s.c. results gave indirect evidence that, upon poling, the most stable ferroelectric phase with nearly perfect all-*trans* conformation is transformed to the unstable ferroelectric phase with some *gauche* defects resulting from the imperfect propagation of dipole rotation along the chain due to the large steric hindrance against dipole rotation, whereas the less stable ferroelectric phase with considerable *gauche* defects along the chain shows a reduction of *gauche* defects through structural reorganization by dipole rotation. The total enthalpy of the Curie transition was greater for all samples after poling. From X-ray diffraction, the average ferroelectric domain size was found to increase in the direction perpendicular to the chain axis upon poling. These results suggest that all samples show increases in the average packing density, the total amount of *trans* conformers and the degree of ferroelectric crystallinity, irrespective of the initial content of ferroelectric phases of different thermodynamic stability present in the sample prior to poling. From vibrational spectroscopies, however, clear evidence that the total amount of *trans* conformers increases and the *gauche* defects are reduced upon poling was not found. No significant differences in the average degree of dipole orientation after poling were observed between the samples from i.r. absorbance spectra in the CH_2 stretching vibration region. This indicates that, contrary to expectation, the most important factor in obtaining the highest degree of dipole orientation, i.e. the highest piezoelectric constant, is not the thermodynamic stability of the ferroelectric phase present in the sample.

(Keywords: VDF/TrFE copolymer; Curie transition; ferroelectric crystal structure; poling; consecutive annealing in the ferroelectric state; X-ray diffraction; d.s.c.)

INTRODUCTION

Vinylidene fluoride(VDF)–trifluoroethylene(TrFE) copolymer [P(VDF/TrFE)] with VDF content between 50 and 80 mol% forms a ferroelectric β-phase directly on crystallization from the melt without any further stretching, and shows higher piezoelectricity than PVDF which is used widely as a polymeric piezoelectric material[1–8]. The ferroelectric-to-paraelectric transition, that is, the Curie transition, is observed in this copolymer[1–8]. The chain conformation of the copolymer is all-*trans* planar zigzag in the ferroelectric phase, while the paraelectric phase above the Curie transition is known to be helical, containing a number of *gauche* linkages. Since the microstructure of these copolymers is strongly perturbed by processing conditions, a considerable amount of *gauche* isomers can be introduced even in the ferroelectric phase. The copolymer samples, prepared by slow cooling from the melt or prolonged annealing above the Curie transition, have more content of ferroelectric phase, but the ferroelectric phase is less perfect, thermodynamically less stable, and includes more *gauche* defects when compared with the copolymer samples prepared by rapid cooling from the melt[9–11].

In our latest study[12], the ferroelectric crystal phase with the least *gauche* defects and the greatest thermodynamic stability, showing a significantly increased Curie transition point, could be obtained by consecutive annealing below the Curie transition. It was found that the ferroelectric phase having a higher Curie transition point has more *trans* sequences and less *gauche* defects, closer packing, shorter intermolecular spacing, and larger thickness of the crystallite along the chain axis.

* To whom correspondence should be addressed
† Permanent address: Kohap Ltd, Euwang-si, Kyunggi-do 437-010, Republic of Korea

More enthalpy was required for the Curie transition that occurred at higher temperatures.

It is also known that chain conformation, packing and macroscopic electric response can change significantly in the presence of an electric field[13–19]. An understanding of field-induced structural changes is of importance in order to establish the molecular mechanisms associated with the macroscopic electrical properties. However, only a few research groups[20–25] have studied changes in the degree of dipole orientation in the presence of an applied electric field. The coupling of CF_2 dipoles with the electric field, i.e. the rotation of dipoles in the direction of the electric field, is also expected to produce structural changes of different levels. For example, the sequence length of specific conformations, packing of segments in the crystalline unit cell, degree of crystallinity, individual dipole orientation and the overall segmental orientation are all influenced by the electric field[6,13,15,20–25]. All of these structural changes directly influence the overall electrical properties of VDF polymers.

Büchtemann *et al.*[20–23] calculated the mean dipole orientation in highly oriented PVDF films subject to an electric field from the absorbances of the infrared bands at 510 and 445 cm^{-1}. Day *et al.*[24] obtained direct evidence supporting the six-site model dipolar orientation in the ferroelectric phase of P(VDF/TrFE) on poling from wide-angle X-ray diffractometry. However, they did not find any changes in crystallinity, chain conformation or segmental chain orientation, which may be produced cooperatively in the presence of the field by the rotation of CF_2 dipoles. In our previous paper[25], upon the application of an electric field of 1.0 MV cm^{-1} to a 75/25 VDF/TrFE copolymer film that was uniaxially drawn and then annealed above the Curie transition temperature, the mean-squared cos α value with respect to the film plane of the CH_2 dipoles in the crystalline domain was found to change irreversibly from 0.46 to 0.34, as recorded by infrared spectroscopy. Additionally, the first observation of an increase in the degree of crystallinity of approximately 8% and the reduction of *gauche* defects on poling was also reported.

As no electric response is observed in the amorphous phase and only the CF_2 dipole in the crystalline phase can react with an external electric field[16,25], annealing to increase the crystallinity must be performed above the Curie transition temperature prior to poling to produce a highly electroactive sample. Kim *et al.*[26] showed that changes in the crystallinity could be monitored quantitatively as a function of annealing temperature by factor analysis and that the crystallinity could be significantly increased by annealing only above the Curie transition point. Tajitsu *et al.*[16] showed that annealing above the Curie transition temperature increased significantly the remnant polarization due to an increase in crystallinity. Koga and Ohigashi[15] revealed, on the basis of X-ray diffraction, that poling increased the crystallinity and size of the crystallites in the ferroelectric phase and especially reduced imperfections or defects in the crystallites.

All VDF/TrFE copolymer samples which have been used to date in investigating ferroelectricity, electroactivity or piezoelectricity have a considerable amount of ferroelectric crystalline defects, i.e. *gauche* conformational defects due to annealing in the paraelectric state above the Curie transition temperature. It is of interest to ascertain whether the same results as shown in previous papers[15,25] can be expected when we apply the same poling procedures to a perfect ferroelectric crystalline sample. We focus our attention on verifying how the effects of poling on the chain conformation, ferroelectric crystalline structure and Curie transition behaviour vary between samples with various levels of *gauche* conformational defects in the ferroelectric state. Consecutive annealing in the ferroelectric state was used to prepare three samples with extremely different amounts of ferroelectric crystalline defects, as proposed in the previous paper[12].

EXPERIMENTAL

Films of P(VDF/TrFE), molar ratio 75/25, were cast from 5% acetone solution onto glass Petri dishes, quickly transferred to the drying oven maintained at 50°C, dried for 1 h, and further dried under vacuum for a day. The film was peeled off the glass at room temperature. The thickness was *ca.* 30 μm. We prepared three samples with extremely different amounts of ferroelectric crystalline defects as follows. The as-cast film was annealed in a vacuum oven at 135°C for 12 h to obtain as high a crystallinity as possible. After that the sample was taken out and cooled as usual to room temperature. It was then kept in a vacuum desiccator before a consecutive annealing in the ferroelectric crystalline state was performed. *Figure 1A* shows the d.s.c. thermogram of an as-annealed sample, coded as F0. The F0 sample was annealed consecutively in the ferroelectric crystalline state with increasing consecutive annealing temperature, as proposed in the previous paper[12]. The annealing time was set as 2 h for each consecutive annealing step. As the consecutive annealing temperature was increased repeatedly from 100°C up to 113°C to obtain as stable a ferroelectric crystalline phase as possible, the Curie transition peak became sharper and shifted to higher temperatures, maintaining a single peak. Each consecutive annealing temperature was chosen to be 2 or 3°C lower than the onset temperature of the Curie transition that the sample showed before the next consecutive annealing was carried out. The Curie transition temperature was elevated drastically and discontinuously at the consecutive annealing temperature of 114°C and a new broad endothermic peak

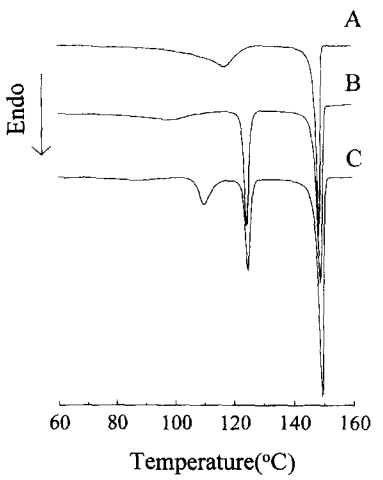

Figure 1 D.s.c. thermograms of P(VDF/TrFE) containing various levels of ferroelectric crystalline defects: (A) F0; (B) F1; (C) F2

appeared at 100°C, as shown in *Figure 1B*. This sample was coded as F1. The sample coded as F2 was obtained after the F1 sample was annealed again at 100°C for 2 h. The d.s.c. thermogram of the F2 sample is shown in *Figure 1C*.

Poling was achieved by placing the sample film between aluminium foil electrodes. All poling experiments were carried out in a silicon bath to prevent electric breakdown with the maximum field of 0.9 MV cm^{-1} at room temperature and 70°C. Thermal analysis was performed using a Perkin-Elmer DSC-4 at a heating rate of 10°C min^{-1} from 50 to 170°C. To investigate the changes in chain conformation and dipole orientation in the ferroelectric crystalline phase upon poling, i.r. spectra were recorded on a Brüker IFS 66 spectrometer with a resolution of 2 cm^{-1} and a scan number of 32. Raman spectra were recorded on a Perkin-Elmer FT-Raman spectrometer (system 2000) with a resolution of 4 cm^{-1} and a scan number of 70. Laser excitation was supplied by the 1064 nm line of an Nd:YAG laser at 1000 mW. X-ray measurements were carried out in reflection mode on a Siemens X-ray diffractometer (model D5000) with a Kevex detector. Step scanning was carried out at 0.05° intervals and 4 s counting time per step. Ni-filtered Cu K_α radiation was used as the X-ray source.

RESULTS AND DISCUSSION

D.s.c. analysis of microstructural changes as a function of poling

As the Curie transition is a crystalline phase transition, its behaviour is highly dependent on the thermodynamic stability of each crystalline phase. *Figure 2* depicts the chemical potential vs temperature for ferroelectric, paraelectric and melt phases, where μ_F, μ_P and μ_M stand for the chemical potential of each phase, respectively. The Curie transition temperature (T_c) is the intersecting point of the μ_F and μ_P lines, whereas the melting point is the intersection of the μ_P and μ_M lines. Higher annealing or crystallization temperature and/or longer annealing time above T_c yields lamellar thickening, better crystalline packing, less defects and higher crystallinity of the paraelectric phase, which results in a downward shift of the μ_P line. Consequently, increase in the melting temperature and depression of T_c are expected. This expectation was experimentally proven to be true in some studies[9,11]. When the same concept is applied to annealing in the ferroelectric state, an increase of the Curie transition point due to the downward shift of the μ_F line without any shift of the μ_P line is expected. This expectation was also proven to be true in a previous paper by our group[12]. We applied annealing in the ferroelectric state to prepare samples having various thermodynamic stabilities, i.e. various ferroelectric crystalline defects.

The broad endothermic peak centred at 118°C of the as-annealed F0 sample, shown in *Figure 1A*, corresponds to the ferroelectric-to-paraelectric phase (F ⇒ P) transition. Even though the Curie transition is known to be a first-order transition with very large thermal hysteresis[8,27], as in the case of melting transition, the F ⇒ P transition of this sample is rather diffuse, ranging from 85 to 125°C, when compared with the sharp melting transition. This indicates that various kinds of ferroelectric phases

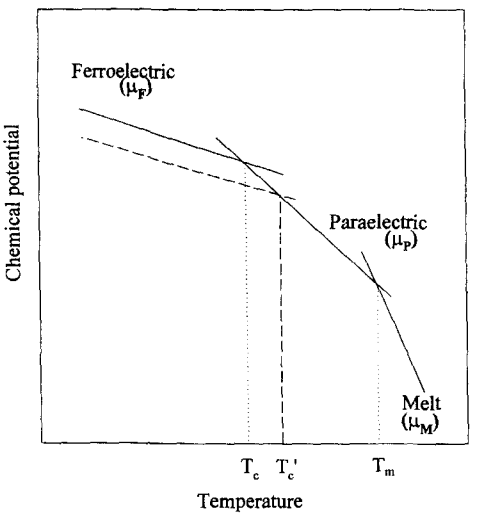

Figure 2 Chemical potential diagrams of the ferroelectric, paraelectric and melt phases of P(VDF/TrFE)

having different thermodynamic stability and/or conformational defects exist in the as-annealed sample. As the consecutive annealing temperature was increased repeatedly from 100°C up to 113°C to obtain as stable a ferroelectric crystalline phase as possible, the Curie transition peak became sharper and shifted to higher temperatures, maintaining a single peak. Each consecutive annealing temperature was chosen to be 2 or 3°C lower than the onset temperature of the Curie transition that the sample showed before the next consecutive annealing was carried out, as in the previous paper[12]. The Curie transition temperature was elevated drastically and discontinuously at the consecutive annealing temperature of 114°C and a new broad endothermic peak appeared at 100°C, as shown in *Figure 1B*. This new broad peak is thought to correspond to the Curie transition of the very unstable ferroelectric phase that is produced due to molecular disordering of the stable ferroelectric phase by excessive thermal energy during annealing. But most of thermal energy was used in transforming the ferroelectric phase into a more stable ferroelectric state. The new unstable ferroelectric phase could be stabilized thermodynamically by further annealing. The F1 sample was annealed again at 100°C for 2 h to make the broad transition centered at 100°C narrower, with little effect on the main Curie transition behaviour. This produced a sample F2 having an additional sharp transition peak centred at 110°C and a very broad transition peak centred at 90°C with the main Curie transition peak at 125°C unchanged, as seen in *Figure 1C*. We designate the ferroelectric crystalline phase exhibiting Curie transition peak temperatures higher than 118°C as the F_α phase, the ferroelectric phase with the Curie transition ranging from 110 and 118°C as the F_β phase, and the ferroelectric phase having the Curie transition temperature lower than 110°C as the F_γ phase.

Even though these three samples have different ferroelectric crystalline phases after consecutive annealing below T_c, they show identical melting transition points and heats of fusion (ca. 7.6 cal g^{-1}). This suggests that they have the same paraelectric crystalline phase after the F ⇒ P transition. Annealing below T_c does not affect the initially formed paraelectric crystalline phase but affects

only the ferroelectric crystalline phase, as predicted by the thermodynamic considerations shown in *Figure 2*. It is very interesting that the ferroelectric phases of different thermodynamic stability, due to different annealing conditions below T_c, can return, through the F ⇒ P transition, to a single paraelectric phase similar to that formed during the first crystallization or annealing above T_c. In conclusion, all of the three transition peaks present below the melting point of the F2 sample correspond to the transition of three different kinds of ferroelectric phases into an identical paraelectric crystalline phase; i.e., $F_\gamma \Rightarrow P$ (very broad transition, 90°C), $F_\beta \Rightarrow P$ (113°C), and $F_\alpha \Rightarrow P$ (125°C). In the previous paper[12] we suggested the possibility of a 'memory effect' in the F ⇒ P transition to interpret this phenomenon.

The structural difference between each ferroelectric phase was clearly elucidated by far-i.r., Raman and X-ray measurements in the previous paper[12]. It was revealed that the ferroelectric phase having the higher Curie transition point has more *trans* sequences and less *gauche* defects, closer packing order, shorter intermolecular spacing, and larger thickness of the crystallite along the chain axis. More enthalpy was required for the Curie transition that occurred at higher temperatures.

Since the electrical property originates only from the crystalline units, information on orientation of individual dipoles along the chain, chain conformation in crystal units, crystalline packing, degree of crystallinity, crystal orientation and crystal size is of importance. For these electrically active polymers, crystal orientation, orientation of individual dipoles along the chain and the relative chain orientation are equally important in determining macroscopic electrical properties. Thus, chain orientation by drawing, crystallization by annealing and CF_2 dipole orientation by poling are needed to achieve high piezoelectric and pyroelectric constants with both PVDF homopolymer and its copolymers. The dipolar orientation can result in a change in chain conformation, microstructural packing density, crystallinity, molecular chain orientation and crystal size during poling. An understanding of such field-induced structural changes is very important in order to establish the molecular mechanisms associated with macroscopic electrical properties.

In a previous paper[25], infra-red spectroscopy was employed to characterize changes in the chain conformation of a 75/25 VDF/TrFE copolymer and orientation of the CF_2 dipoles along the chain as a result of the poling procedure. Upon poling, the degree of crystallinity increased from 0.50 to 0.56, and this was accomplished by a small increase in the number of long sequences of *trans* conformers and a small decrease in the number of crystalline *gauche* conformers. The $\langle \cos^2 \alpha \rangle_{cr}$ value for the CH_2 dipoles in the crystalline region with respect to the film plane was changed from 0.46 to 0.34 after poling, where α is the angle between the CH_2 dipoles and the transverse direction of the film. This change in the $\langle \cos^2 \alpha \rangle_{cr}$ value for the CH_2 dipoles in the crystalline region indicates that these dipoles orient preferentially along the electric field direction upon poling. Büchtemann *et al.*[20–23] showed a similar degree of orientation of CF_2 dipoles for a uniaxially drawn PVDF homopolymer film, on the basis of infra-red spectroscopic results.

The microscopic mechanism of polarization reversal arising in the crystalline region upon poling has not been clarified. Two main models were proposed to explain polarization reversal of the PVDF β-phase. The first model is a 180° rotation of dipolar chains[28–30], and the second is that polarization reversal can also be achieved by successive 60° rotations[31–33]. The 180° rotations can be achieved in two different ways: (1) solitonic propagation of kink structure[28], and (2) simultaneous rotation of all the dipoles in a chain[29]. Recently, the successive 60° rotation step model is accepted as being more plausible and evidenced experimentally[24].

This rotation of the CF_2 dipole along the chain upon poling forms new crystalline domains by changing chain conformation, crystal perfection, crystallinity and crystal size. Irrespective of rotation mechanism, it is expected that the CF_2 dipole rotation initiated by poling cannot propagate completely along the chain in the perfect ferroelectric crystal phase and that all the CF_2 dipoles cannot rotate simultaneously upon poling. This incomplete rotation must produce conformational and packing defects in the crystal lattice. However, no studies on the production of crystal or conformational defects upon poling have been reported to date, because it was impossible to prepare a perfect ferroelectric crystal sample without any conformational or packing defects. On the other hand, Koga and Ohigashi[15] and Kim and Hsu[25] showed that poling increased the overall crystallinity and crystal size and reduced packing and conformational *gauche* defects in the crystallites for stretched or unstretched VDF/TrFE copolymer films annealed above the Curie transition temperature. However, these samples annealed above T_c must be not considered as perfect ferroelectric phases. They contain various kinds of ferroelectric phases having different thermodynamic stability or conformational defects, as indicated in the thermodynamic consideration and d.s.c. result of the F0 sample in *Figure 1A*.

In this study we prepared three samples, F0, F1 and F2, having different compositions of F_α, F_β and F_γ for poling. *Figure 1* shows their Curie and melting transitions. As discussed earlier with regard to *Figure 2*, the higher Curie transition temperature must reflect a higher structural order of the corresponding ferroelectric phase. As revealed in the preceding paper[12], the F_γ phase is the least ordered ferroelectric phase, whereas the F_α phase is the most ordered one. The F_α phase was found to have all-*trans* conformation without the least amount of *gauche* defects along the chain axis, and the F_γ phase was found, by means of far-i.r. and Raman spectroscopies and X-ray diffraction, to have shorter *trans* sequence with many *gauche* defects that are randomly distributed along the chain axis.

The effect of poling on the Curie transition behaviours and chain conformational changes of the three samples F0, F1 and F2 was analysed by d.s.c. analysis. *Figure 3* shows the d.s.c. thermograms of the F0 sample before and after poling. The Curie transition temperature shifted to a slightly higher temperature, the endothermic peak became sharper, and the enthalpy of Curie transition was increased after poling. This indicates that the rotation of the CF_2 dipoles along the chain axis upon poling produces a new ferroelectric crystal phase with increased amounts of the thermodynamically more stable ferroelectric phases due to the reduction of the *gauche* conformational defects included in the ferroelectric phase. This result is identical to several results that two research groups[15,25] have already shown for the

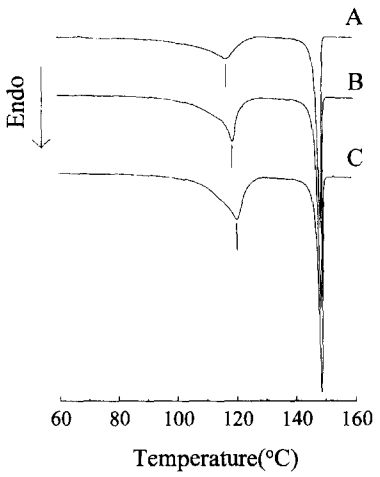

Figure 3 D.s.c. thermograms of the F0 sample as a function of poling: (A) unpoled; (B) poled at room temperature; (C) poled at 70°C

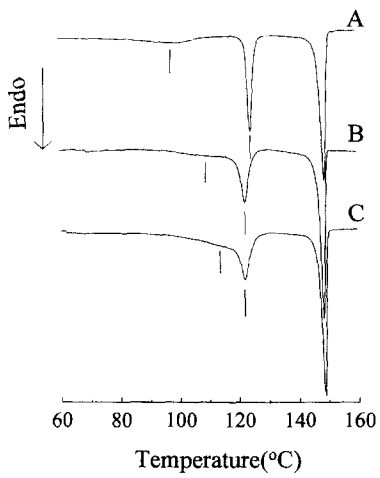

Figure 4 D.s.c. thermograms of the F1 sample as a function of poling: (A) unpoled; (B) poled at room temperature; (C) poled at 70°C

poling of stretched or unstretched VDF/TrFE copolymer films annealed above the Curie transition temperature. In the case of poling at 70°C, the Curie transition temperature and the enthalpy of Curie transition are slightly higher than in samples poled at room temperature. This is attributed to the fact that the activation energy for the rotation of the CF_2 dipole can be overcome more easily at higher temperatures, and that the number of rotated CF_2 dipoles is increased at higher poling temperatures. No changes in melting transition behaviours were observed on poling, which indicates that poling cannot affect the paraelectric crystal phase to which the ferroelectric phase will be transformed above the Curie transition upon heating, but will affect only the ferroelectric crystal phase. It is very interesting that even though ferroelectric phases quite different from the ferroelectric ones present before poling are newly formed upon poling, they can return through the ferroelectric-to-paraelectric phase transition to the initial paraelectric phase formed during annealing above T_c. The 'memory effect', that the conformational information of the initial paraelectric phase can be memorized in the ferroelectric phase even after the paraelectric-to-ferroelectric phase transition, suggested in the preceding

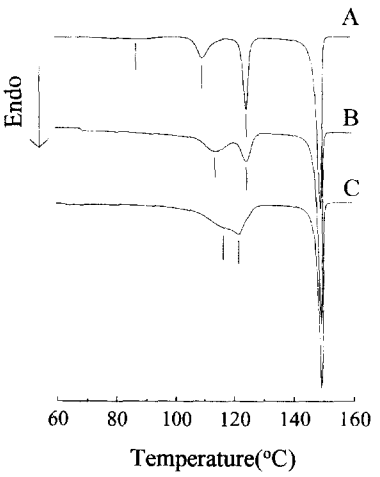

Figure 5 D.s.c. thermograms of the F2 sample as a function of poling: (A) unpoled; (B) poled at room temperature; (C) poled at 70°C

paper[12], can also be applied to the explanation of the melting transition behaviour on poling.

Figure 4 shows d.s.c. thermograms of the F1 sample which initially consists mostly of nearly perfect ferroelectric phase F_α and small amounts of very unstable ferroelectric phase F_γ before and after poling. The F_γ phase was transformed to the F_β phase after poling, whereas the F_α phase was transformed to a thermodynamically less stable F_α phase. As discussed earlier, the higher Curie transition temperature reflects a higher structural order of the corresponding ferroelectric phase and less conformational *gauche* defects in the corresponding ferroelectric phase. Thus, poling increases the amount of *gauche* conformers in the F_α phase having the least amount of conformational defects. This indicates that since the steric hindrance is too large in the perfect ferroelectric phase composed only of all-*trans* conformers for the rotation of the CF_2 dipoles to propagate completely along the whole chain axis or for the CF_2 dipoles of all the neighboring chains to rotate simultaneously, the incomplete propagation of the rotation of the CF_2 dipoles or the incomplete simultaneous rotation of the CF_2 dipoles of the neighbouring chains must yield the conformational *gauche* defects along the chain. On the other hand, poling reduces the *gauche* defects for the F_γ phase. This results from the fact that the increasing intermolecular distance due to the increasing *gauche* conformers can reduce considerably the steric hindrance against the rotation of the CF_2 dipoles, and the propagation of the rotation of the dipoles or the simultaneous rotation becomes easier, and thus poling contributes to the reduction of the *gauche* defects. Increasing the poling temperature increases the enthalpy of the Curie transition and the $F_\beta \Rightarrow P$ transition temperature. Melting transition does not change as a function of poling, as in the case of the poling of the F0 sample.

Figure 5 shows d.s.c. thermograms before and after poling for the F2 sample which has a nearly perfect ferroelectric phase F_α, a slightly unstable ferroelectric phase F_β, and a small amount of the F_γ phase. The F_γ phase disappeared and the F_β phase was transformed to the thermodynamically more stable F_β phase on poling, whereas the F_α phase was transformed to thermodynamically unstable F_α phase. Increasing the poling

Table 1 Summary of d.s.c. results as a function of poling for samples F0, F1 and F2

Sample code	Poling temp.	T_c (°C)	T_m (°C)	ΔH_c (cal g^{-1})	ΔH_m (cal g^{-1})
F0	unpoled	116.8	148.6	5.7	7.8
	room temp.	119.2	148.6	6.4	7.8
	70°C	120.4	148.7	7.8	7.8
F1	unpoled	98.1^{γ}	148.8	1.4^{γ}	7.3
		124.8^{α}		3.7^{α}	
	room temp.	$109.1^{\beta,sh^a}$	148.6	5.3	7.6
		122.4^{α}			
	70°C	$111.1^{\beta,sh^a}$	148.8	6.4	7.5
		122.3^{α}			
F2	unpoled	111.3^{β}	149.2	2.5	7.6
		126.0^{α}		2.1	
	room temp.	113.8^{β}	149.4	5.5	7.6
		125.0^{α}			
	70°C	$116.0^{\beta,sh^a}$	149.5	6.6	7.8
		122.0^{α}			

[a] sh: shoulder

temperature showed these changes more clearly. The more diffuse Curie transition curve of the F_α phase and the shift of the Curie transition peak of the F_α phase to lower temperatures on poling also indicate that the incomplete propagation of dipole rotation along the chain axis or the incomplete simultaneous rotation of the CF_2 dipoles due to the steric hindrance against the rotation of the CF_2 dipoles in the perfect ferroelectric F_α phase yields conformational *gauche* defects along the chain during poling. The disappearance of the Curie transition of the F_γ phase and the shift of the Curie transition peak of the F_β phase to higher transition temperatures also indicate that the *gauche* defects make the CF_2 dipole rotation much easier, due to the reduction of the steric hindrance against the CF_2 dipole rotation. Again, no changes in the melting transition as a function of poling could be observed in this case.

In addition to the changes in Curie transition temperatures on poling, the increases in the enthalpy of Curie transition were clearly observed for all the samples (see *Table 1*). These results are directly related to increases in the average packing density, the total amount of *trans* conformers and the degree of ferroelectric crystallinity due to the reduction of *gauche* defects and/or the formation of ferroelectric phase from the amorphous phase in the ferroelectric crystal interface through the structural rearrangement induced by the propagation of the rotation of CF_2 dipoles along the chain axis upon poling. As discussed above, the F_γ and F_β phases are transformed to the thermodynamically more stable F_β phase upon poling, resulting in a decrease in the amount of *gauche* conformers. On the other hand, the nearly perfect ferroelectric F_α phase in the F1 and F2 samples is transformed to a less stable F_α phase upon poling, which results in increased *gauche* content. However, the increase in the enthalpy of Curie transition on poling indicates that the reduction of *gauche* defects is more dominant than the increase of *gauche* conformers upon poling. The samples poled at 70°C have a higher enthalpy of Curie transition than those poled at room temperature. Even though the as-annealed sample F0 has a less stable ferroelectric phase than the other consecutively annealed samples, it exhibits a higher enthalpy of Curie transition than the other samples. This indicates that the samples which have some *gauche* defects in the ferroelectric crystal can increase the total amount of *trans* conformers more than the other consecutively-annealed samples with fewer *gauche* defects, since the *gauche* defects make the propagation of the CF_2 dipole rotation along the chain much easier due to the reduction of the potential energy barrier against CF_2 dipole rotation. This result is very consistent with the previous report[25] concluding that, upon poling, the degree of crystallinity increased, and that this was accompanied by a small increase in the number of long sequences of *trans* conformers. The changes in the d.s.c. results as a function of poling are summarized in *Table 1*.

X-ray diffraction analysis of microstructural changes as a function of poling

The rotation of the CF_2 dipole induced by poling must reorganize the ferroelectric crystal phase. Thus, this structural reorganization of the ferroelectric phase is expected to result in changes in the size, interplanar distance or packing density of the ferroelectric crystalline lattice. These changes can be detected by X-ray diffraction. When d.s.c. results are considered, it is not difficult to expect that poling, which improves the packing density or increases the perfection of the crystalline region, can also change the X-ray diffraction pattern. Since X-ray diffraction gives information about the composite crystalline structures rather than individual crystalline information of the individual ferroelectric phases present in the sample, it is not easy to elucidate how each individual ferroelectric phase responds to an electric field. *Figure 6* shows X-ray diffractograms of the F2 sample before and after poling. The (200)/(110) diffraction peak at around 20° became very sharp and the broad shoulder on the low-angle side of this peak ($2\theta = 18.3°$), corresponding to diffraction from the amorphous regions, nearly disappeared on poling. The other F0 and F1 samples also showed similar behaviour upon poling. From X-ray diffraction results as a function of poling, one cannot observe as significant a difference among the three samples as shown from d.s.c. results.

The coherence length L_c in the crystallites was

calculated from the FWHM using the Scherrer formula

$$L_c = \frac{0.9\lambda}{\text{FWHM} \cdot \cos\theta_B}$$

where λ is 1.5406 Å, FWHM is the full width at half maximum (in rad), and θ_B is the Bragg angle. X-ray diffraction results are summarized in *Table 2*. The (200) and (110) Bragg reflections shifted to a slightly higher angle and the thickness of crystallite perpendicular to the chain axis increased by more than two times on poling. These results can be interpreted as follows. The reduced lattice expansion due to the reduction of *gauche* defects decreases the interchain distance, and the increasing domain size of the reorganized ferroelectric phase along the lateral direction increases the coherence length. Drastic reduction of diffraction from the amorphous regions indicates the occurrence of field-induced crystallization upon poling, as predicted from d.s.c. results. Diffractions at 35.2° are assigned to the Bragg reflections of (001), (020) and (310)[24]. While, in the case of a uniaxially drawn sample, (020) and (310) reflections are observed in the equatorial scan and (001) reflection occurs in the meridional scan, all of these reflections occur at 35.2° even in the equatorial scan of an unoriented as-annealed sample.

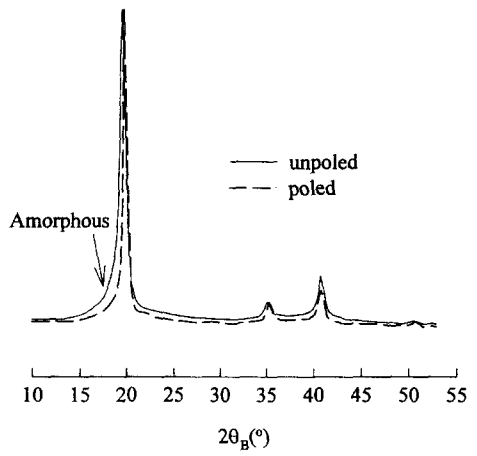

Figure 6 X-ray diffractograms of the F2 sample before and after poling. Poling temperature: 70°C

The contribution of each plane to the observed intensity of the diffraction peak at 35.2° can be estimated using the structure factor for each diffraction. The calculated intensities of (001), (020) and (310) reflections are 310, 432 and 221, respectively[24]. The Bragg reflection of 35.2° shifted to a slightly higher angle after poling, which resulted from the reduction of *gauche* defects. The increase in the crystallite thickness was not so great as compared with the (200)/(110) reflection. For the (201)/(111) diffraction at 40.85°, only the increase in the crystallite thickness is observed without changes in peak positions on poling. This reflection at 40.85° is also mixed with (400) and (220) equatorial reflections. Since the calculated intensities of (201) and (220) reflections are negligibly small and the contribution of (400) reflection to the total intensity is about one-third of that of the (111) reflection, the change in the reflection peak at

Table 2 Summary of X-ray diffraction results as a function of poling[a] for samples F0, F1 and F2

		(200)/(110)	(001)	(201)/(111)
			(310)/(020)	(400)/(220)
F0	*Before poling*			
	$2\theta_B$ (°)	19.88	35.20	40.85
	Planar spacing (Å)	4.462	2.548	2.207
	Crystal thickness (Å)	153	192	120
	After poling			
	$2\theta_B$ (°)	20.06	35.42	40.80
	Planar spacing (Å)	4.423	2.253	2.210
	Crystal thickness (Å)	369	266	200
F1	*Before poling*			
	$2\theta_B$ (°)	19.91	35.20	40.84
	Planar spacing (Å)	4.456	2.548	2.208
	Crystal thickness (Å)	157	205	156
	After poling			
	$2\theta_B$ (°)	20.07	35.42	40.84
	Planar spacing (Å)	4.421	2.532	2.208
	Crystal thickness (Å)	346	223	216
F2	*Before poling*			
	$2\theta_B$ (°)	19.94	35.21	40.86
	Planar spacing (Å)	4.449	2.547	2.207
	Crystal thickness (Å)	169	225	175
	After poling			
	$2\theta_B$ (°)	20.05	35.40	40.81
	Planar spacing (Å)	4.424	2.534	2.209
	Crystal thickness (Å)	361	214	225

[a] Poling temperature: 70°C

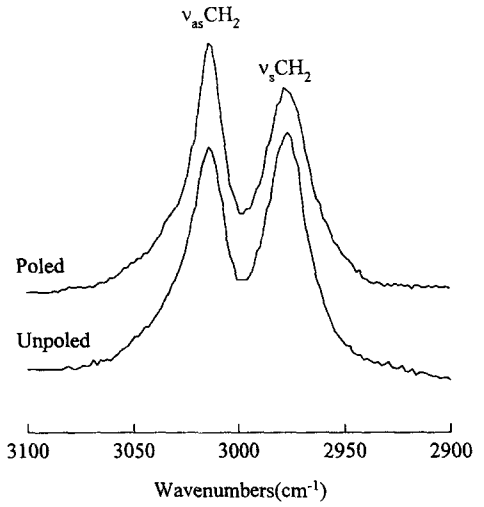

Figure 7 Infra-red spectra of the F0 sample before and after poling in the CH_2 stretching region. Poling temperature: 70°C

40.85° on poling can be attributed mainly to the change in the (111) reflection. All of these results, however, are inconsistent with Day *et al.*'s X-ray result[24] that poling does not improve the packing of the crystalline segments or increase the perfection of the crystalline regions.

Vibrational spectroscopic analysis of microstructural change as a function of poling

The piezo- and pyroelectricity of PVDF and VDF/TrFE copolymers are highly related to the crystallinity, thermodynamic stability of ferroelectric phase, chain orientation, and the degree of CF_2 dipole orientation toward the electric field. This study was started on the basis of expectations that, since only the ferroelectric phase is polar and electroactive, the sample with higher amounts of ferroelectric crystal and more stable ferroelectric phase will have greater piezo- and pyroelectricity. The as-cast sample was annealed at 135°C for 12 h to obtain as high a crystallinity as possible, and then the as-annealed sample was annealed consecutively at temperatures below the Curie transition point to obtain a thermodynamically more stable ferroelectric crystal, i.e. the ferroelectric crystal with the fewest *gauche* conformers. Mechanical orientation is usually used to obtain better chain orientation and greater amount of electroactive β phase for PVDF. An electroactive ferroelectric phase of P(VDF/TrFE) can be obtained without mechanical orientation just by cooling below the Curie transition point after crystallization or annealing. Finally, a poling process is necessary to align the CF_2 dipoles in the electric field direction to achieve piezo- and pyroelectricity.

The three samples F0, F1 and F2 used in this study have identical crystallinity, but consist of crystals of various levels of thermodynamic stability (F_α, F_β and F_γ) in the ferroelectric state. As discussed with the d.s.c. results, the F_γ and F_β phases having a considerable quantity of *gauche* defects are transformed to thermodynamically more stable ferroelectric phase containing fewer *gauche* defects through poling, but the F_α phase is transformed rather to a less stable ferroelectric phase. Therefore, it is not easy to predict which sample will have the highest degree of CF_2 dipole orientation after poling.

Infra-red spectroscopy has been used widely to estimate the degree of dipole orientation[20–23,25]. The CH_2 symmetric (2987 cm^{-1}) and asymmetric (3012 cm^{-1}) stretching vibrations can be employed for dipolar orientation analysis[25], because CH_2 dipoles are opposite to CF_2 dipoles, their stretching vibrations are isolated vibration mode, not related to the chain conformational change, and their transition moments can be assumed to be perpendicular to the chain axis. *Figure 7* shows infra-red spectra of the F0 sample before and after poling in the CH_2 stretching region. Both the CH_2 symmetric and asymmetric stretching vibrations are readily seen to change significantly in the presence of the electric field. The ratio of absorbance at 3012 cm^{-1} to one at 2987 cm^{-1} (A_{3012}/A_{2987}) was used to calculate the average degree of dipole orientation in a previous paper[25]. The greater value of this ratio shows the higher degree of dipole orientation toward the electric field. Unfortunately, since the individual CH_2 stretching vibration peaks of each ferroelectric phase cannot be obtained separately as a function of a poling, it was impossible to elucidate which ferroelectric phase could have a higher degree of dipole orientation toward the field direction. One can estimate only the average dipole orientation of the sample rather than the individual dipole orientation of each ferroelectric phase by i.r. measurement. No significant differences in the ratio A_{3012}/A_{2987} between the three samples were observed on poling. This indicates that they may have identical macroscopic electrical properties because they have nearly identical average dipole orientation on poling even though they have various levels of thermodynamic stability in the ferroelectric state before poling. Contrary to our expectations in the previous study[25], consecutive annealing in the ferroelectric state does not seem to be a good method of improving the piezo- and pyroelectricity.

Infra-red spectroscopy in another frequency region can also be used to investigate the chain conformation and dipole orientation changes as a function of poling. In the poled F0 sample, the reduction of intensity at 1290 ($\nu_SCF_2 + \nu_SCC + \delta_SCCC$, long-*trans* sequence, $t_m(m > 4)$) and 848 ($\nu_SCF_2 + \nu_SCC$, $t_m(m > 3)$) cm^{-1} and the increase of intensity at 884 ($\rho CH_2 + \nu_{as}CF_2 + \rho CF_2$, $t_m(m > 1)$) cm^{-1} were observed and there was no significant change in the intensity at 602 (crystalline *tg*) cm^{-1}. With these changes, however, one cannot conclude that the poling process can increase or decrease the amount of *trans* conformers, because these bands are highly dependent on the degree of dipole orientation as well as the amount of *trans* isomers or *gauche* isomers. For example, the intensity at two *trans* bands (1290 and 884 cm^{-1}) is reduced, but the intensity at another *trans* band (884 cm^{-1}) is increased upon poling. This contrary result is attributed to the fact that i.r. bands can be highly dependent on the degree of orientation toward the electric field as well as the amount of the corresponding functional group[14,25]. The differences in intensities at 1290, 884, 848 and 602 cm^{-1} were not observed between the three poled samples. Also no significant differences were observed in Raman spectra in the 1500–100 cm^{-1} region. These results indicate that the three samples may have nearly identical amounts of *trans* and *gauche* conformers and identical average degree of dipole orientation after poling, irrespective of consecutive annealing conditions in the ferroelectric state, if they are annealed at the same condition above the Curie transition point.

CONCLUSION

In order to observe how differently a perfect ferroelectric phase and an imperfect ferroelectric phase respond to an external electric field upon poling, we prepared three typical samples that have different amounts of three kinds of ferroelectric phases (F_α, F_β and F_γ) by consecutive annealing below the Curie transition point, and then poled them at a field strength of 0.9 MV cm^{-1}. The following conclusions can be drawn from the d.s.c., X-ray diffraction, i.r. and Raman scattering results of the poled samples. Upon poling, the perfect ferroelectric phase with all-*trans* conformation is transformed to the less perfect ferroelectric phase with some *gauche* defects resulting from the imperfect propagation of dipole rotation along the chain due to large steric hindrance against dipole rotation, but the less perfect ferroelectric phase with considerable *gauche* defects along the chain shows a reduction in *gauche* defects. The Curie transition point of the most stable F_α phase is lowered on poling, whereas those of the less stable F_β and F_γ phases are shifted to much higher temperatures. The total enthalpy of Curie transition was increased for all the samples.

From X-ray diffraction, the average ferroelectric domain size was found to increase in the direction perpendicular to the chain axis after structural reorganization upon poling. All the samples show increases in the average packing density, the total amount of *trans* conformers and the degree of ferroelectric crystallinity, irrespective of the initial contents of F_α, F_β and F_γ phases present in the sample before poling. From vibrational spectroscopies, however, clear evidence that the total amount of *trans* conformers increases and that of *gauche* defects is reduced upon poling was not found, because the vibrational spectra can change with the degree of dipole orientation as well as the amount of *trans* or *gauche* conformers. No significant differences in the average degree of dipole orientation could be found among the samples from the i.r. absorbance spectra in the CH_2 stretching vibration region, which indicates that the most important factor in obtaining the highest degree of dipole orientation, i.e. the highest piezoelectric constant, is the total amount of electroactive ferroelectric phases rather than the amount of the most stable ferroelectric phases present in the sample.

ACKNOWLEDGMENT

This work was supported by the Korea Science and Engineering Foundation (KOSEF) under grant KOSEF 921-1000-011-2.

REFERENCES

1. Tashiro, K., Takano, K., Kobayashi, M., Chatani, Y. and Tadokoro, H., *Polym. Commun.*, 1981, **22,** 1312.
2. Tashiro, K., Takano, K., Kobayashi, M., Chatani, Y. and Tadokoro, H., *Polymer*, 1984, **25,** 195.
3. Tashiro, K., Takano, K., Kobayashi, M., Chatani, Y. and Tadokoro, H., *Ferroelectrics*, 1984, **57,** 297.
4. Lovinger, A. J., Furukawa, T., Davis, G. T. and Broadhurst, M. S., *Polymer*, 1983, **24,** 1225.
5. Lovinger, A. J., Furukawa, T., Davis, G. T. and Broadhurst, M. S., *Polymer*, 1983, **24,** 1233.
6. Davis, G. T., Furukawa, T., Lovinger, A. J. and Broadhurst, M. S., *Macromolecules*, 1982, **15,** 323.
7. Legrand, J. F., *Ferroelectrics*, 1989, **91,** 303.
8. Tashiro, K. and Kobayashi, M., *Phase Transitions*, 1989, **18,** 213.
9. Stack, G. M. and Ting, R. Y., *J. Polym. Sci., Polym. Phys. Ed.*, 1988, **26,** 55.
10. Tanaka, H., Yukawa, H. and Nishi, T., *Macromolecules*, 1988, **21,** 2469.
11. Kim,. K. J. and Kim, G. B., *J. Appl. Polym. Sci.*, 1993, **47,** 1781.
12. Kim, K. J., Kim, G. B., Vanlencia, C. L. and Rabolt, J. F., *J. Polym. Sci., Polym. Phys. Ed.*, 1994, **32,** 2435.
13. Reynolds, N. M., Kim, K. J., Chang, C. and Hsu, S. L., *Macromolecules*, 1989, **22,** 1092.
14. Kim, K. J., Reynolds, N. M. and Hsu, S. L., *J. Polym. Sci., Polym. Phys. Ed.*, 1993, **31,** 1555.
15. Koga, K. and Ohigashi, H., *J. Appl. Phys.*, 1986, **57,** 2142.
16. Tajitsu, Y., Ogura, H., Chiba, A. and Furukawa, T., *Jpn. J. Appl. Phys.*, 1987, **26,** 554.
17. Furukawa, T., Wen, J. X., Suzuki, K., Takashina, Y. and Date, M., *J. Appl. Phys.*, 1984, **56,** 829.
18. Ohigashi, H. and Koga, K., *Jpn. J. Appl. Phys.*, 1982, **21,** L455.
19. Newman, B. A., Yoon, C. H. and Scheinbeim, J. I., *J. Appl. Phys.*, 1979, **50,** 6095.
20. Büchtemann, A., Stark, W. and Geiss, D., *Acta Polym.*, 1988, **39,** 171.
21. Büchtemann, A. and Geiss, D., *Polymer*, 1991, **32,** 215.
22. Büchtemann, A. and Schmolke, R., *J. Polym. Sci., Polym. Phys. Ed.*, 1991, **29,** 1299.
23. Büchtemann, A., Stark, W. and Künstler, W., *Vib. Spectrosc.*, 1993, **4,** 231.
24. Day, J. A., Lewis, E. L. and Davies, G. R., *Polymer*, 1992, **33,** 1571.
25. Kim, K. J. and Hsu, S. L., *Polymer*, 1994, **35,** 3612.
26. Kim, K. J., Reynolds, N. M. and Hsu, S. L., *Macromolecules*, 1989, **22,** 4395.
27. Koizumi, N., Haikawa, N. and Habuka, H., *Ferroelectrics*, 1984, **57,** 99.
28. Dvey-Aharon, H., Slukin, J. J., Taylor, P. L. and Hopfinger, A. J., *Phys. Rev.*, 1980, **B21,** 3700.
29. Aslaksen, E. W., *J. Chem. Phys.*, 1972, **57,** 2358.
30. Furukawa, T., Date, M. and Johnson, G. E., *J. Appl. Phys.*, 1983, **54,** 1540.
31. Kepler, R. G. and Anderson, R. A., *J. Appl. Phys.*, 1978, **49,** 1232.
32. Hayashi, S. and Imamura, A., *J. Polym. Sci., Polym. Phys. Ed.*, 1992, **30,** 769.
33. Broadhurst, M. G. and Davis, G. T., *Annu. Rep. Conf. Electr. Insul. Diel. Phen.*, 1979, **48,** 447.